Desalination and Water Treatment
www.deswater.com

doi: 10.5004/dwt.2023.29526

295 (2023) 18–29
May

Preparation of high alkalinity polymer ferric sulfate flocculant by new bipolar membrane electrodialysis reactor

Dong Wang, Xiaoyi Li, Yuting Wu, Shaoxiang Li*, Yuqi Zheng, Dan Chen, Nan Zhang, Yueyuan Zhu, Congjie Gao

College of Environment and Safety Engineering, Qingdao University of Science and Technology, Qingdao 266042, China, emails: leeshaoxiang@126.com (S. Li), wd_charrel@163.com (D. Wang), lxy6331@foxmail.com (X. Li), Stella_Wu1@163.com (Y. Wu), marcella_Zheng@163.com (Y. Zheng), xiaoya5868@sina.com (D. Chen), zhangnan_2012@163.com (N. Zhang), 19863816112@163.com (Y. Zhu), geboyang@lnyk.net (C. Gao)

Received 5 October 2022; Accepted 3 April 2023

ABSTRACT

The flocculating ability of the flocculant directly affects the quality of the treated water. Poly-ferric sulfate flocculant (PFS) is a commonly used flocculant. The purpose of this study is to use the electrodialysis process to concentrate the solution and the bipolar membrane electrodialysis to dissociate water to produce acid and alkali to achieve the preparation of poly-ferric sulfate flocculant. The effects of current density, feed flow rate, and sulfuric acid addition on the quality of PFS were tested. Experiments have proved that the increase of current density is beneficial to the increase of PFS alkalinity and turbidity removal rate, and at the same time energy consumption will be reduced. When the current density is 30 mA/cm^2, the alkalinity reaches a maximum of 21.04% and the energy consumption is 1.52 kW·h (kg H_2SO_4). When the current density is 20 mA/cm^2, the turbidity removal rate reaches a maximum of 94.23% and the energy consumption is 2.46 kW·h (kg H_2SO_4). In addition, the solid PFS was subjected to scanning electron microscopy, X-ray diffraction and Fourier-transform infrared spectroscopy tests after vacuum drying to further confirm the structure of the PFS.

Keywords: Poly-ferric sulfate flocculant; Electrodialysis; Bipolar membrane electrodialysis; Coagulation efficiency

1. Introduction

Poly-ferric sulfate (PFS), as described by the chemical formula $[Fe_2(OH)_n(SO_4)_{3-n/2}]_m$, plays a key role in environmental protection. As one of the inorganic polymer coagulants, the molecular weight of PFS is as higher as 10^5 [1]. The significant advantage of PFS is that the hydrolysis of iron ions occurs under specific experimental conditions during the preparation stage of the coagulant and not after their addition to the wastewater [2]. The performance, capacity and stability of flocculants directly affect the water quality after flocculation, so it is important to study and prepare safe, harmless, efficient and effective flocculants [3].

During the last 20 y, a considerable attention has been paid to the pre-hydrolysed inorganic coagulants based on iron, such as polyferric chloride (PFC) or poly-ferric sulfate (PFS). However, the range of iron species formed is influenced by several factors, such as temperature, pH, etc. The traditional preparation method of PFS is direct oxidation, and the oxidizing agents including H_2O_2, $NaClO_2$, $NaClO_3$, and HNO_3, etc [4]. According to the report, the best oxidizer is $NaClO_3$, which can oxidize ferrous ions into iron ions without producing harmful gases such as NO, NO_2, and Cl_2 in the reaction process. Furthermore, $NaClO_3$ has better stability and easy to store and transport compared to H_2O_2. With the deepening of research, people gradually

* Corresponding author.

found that the reaction process of PFS preparation is as follows [5,6]:

Oxidation:

$$8FeSO_4 + 3H_2SO_4 + NaClO_3 \rightarrow 3Fe_2(SO_4)_3 + NaCl + 3H_2O$$

Hydrolysis:

$$Fe_2(SO_4)_3 + nOH^- \rightarrow Fe_2(OH)_n(SO_4)_{3-n/2} + n/2SO_4^{2-}$$

Polymerization:

$$mFe_2(OH)_n(SO_4)_{3-n/2} \rightarrow [Fe_2(OH)_n(SO_4)_{3-n/2}]_m$$

Although the direct oxidation process has become increasingly mature, the biggest deficiency of the method is that the Fe^{2+} is oxidized to Fe^{3+} and then forming $Fe(OH)_3$ precipitates under alkaline conditions, resulting in a decrease in the purity of the finally prepared flocculant [7]. To solve the problem, Ma [8] proposed that if the Fe^{3+} generated in the oxidation stage enter to the hydrolysis stage and the polymerization stage as soon as possible will reduce the Fe^{3+} activity and then the formation of $Fe(OH)_3$ precipitates will be avoided. The difficulty of this method is that the reduction of Fe^{3+} activity will inevitably lead to a decrease in the total iron content of the product. On the other hand, they proposed that another way to solve this problem is to reduce the activity of OH^- by adding more sulfuric acid, which inevitably leads to a decrease in the basicity of the PFS product. Therefore we need to find a new method to overcome the shortcomings of the existing methods.

Electrodialysis (ED) is anion-exchange membrane technique for desalting and concentrating electrolyte solutions under the influence of an electrical potential difference [9]. Bipolar membrane electrodialysis (BMED) is a water treatment technology developed based on electrodialysis technology.

Compared to ED stack, BMED stack can effectively splits water into OH^- and H^+ under an applied electric field thus separating cations and anions to different compartments and converting salt to the corresponding acids and bases [10].

BMED has been widely used in chemical industry, biotechnology, food processing, and environmental protection [10,11]. Shi et al. [12] developed two-phase electro-electrodialysis (TPEED) for recovering and concentrating citric acid. Zhang et al. [13] have proposed a four-compartment BMED configuration to prepare highly pure tetrapropyl ammonium hydroxide and di-quaternary ammonium hydroxide. Miao et al. [14] studied the preparation process of niacin with high yield, low energy consumption and cleaner pollution by using bipolar membrane stack. All process preparations revolve around the use of OH^- and H^+ generated by the bipolar membrane stack due to water decomposition to prepare the corresponding acid or base.

In order to expand the application range of BMED, Li et al. [15] proposed the preparation of PFS by BMED system, using BP-A configuration, and preparing PFS under the experimental conditions of current density 20 mA/cm^2, the PFS basicity achieved to 14.72%. Even though the products, prepared by Zhang's method have reached the requirements of GB14591-2016, the concentrations of Cl^- and ClO_3^- were out of control. The excess ClO_3^- and Cl^- in the products made the water treated with the product still not directly drinkable. In addition, the corrosiveness of Cl^- can cause damage to water supply equipment. Moreover, in this membrane reactor configuration, H^+ and OH^- are generated in the middle layer of the bipolar exchange membrane under the action of electric field, OH^- will bond with Fe^{2+}/Fe^{3+} and adhere to the membrane surface, which will lead to serious Fe^{2+}/Fe^{3+} loss and membrane pollution.

In order to solve these problems, we have proposed a new technology for preparing PFS using ED technology. It mainly includes two steps. First, the concentration function of electrodialysis technology is used to prepare a high-concentration Fe^{2+} and ClO^{3-} initial solution. This solution is called "raw solution" in the experiment. At the same time, through the ED process, the transfer of Na^+ in the oxidant is achieved, which will effect of cations on the stability of the product [16]. Then, the new BMED membrane stack configuration was used to synthesize PFS, the bipolar membrane stack is no longer only converts the salt solution into the corresponding acid or base solution in the traditional sense, but allows the H^+ and OH^- produced by BPM to participate in the oxidation reaction and hydrolysis reaction of the Fe^{2+} ion. The method balances the speed of oxidation reaction and hydrolysis reaction, and reduces the content of Fe^{2+} and Cl^- in the product. This is because CM can hinder the migration of anions and improve the alkalinity and purity of the product. In this article, this concept is called "new bipolar membrane electrodialysis reactor".

In this article, the oxidation and hydrolysis of Fe^{3+} are divided into two parts to carry out the reaction. The first step is to promote the oxidation of Fe^{2+} to Fe^{3+} by using the concentrated solution prepared in the H^+ acidizing electrodialysis process resulting from the hydrolysis of bipolar membranes, and then Fe^{3+} migrate to the alkali compartment for hydrolysis, a high-purity PFS flocculant is obtained. In this study, PFS preparation process integrated with BMED was investigated. The generated liquid PFS was characterized in terms of typical properties, such as pH (1%, sol), density, basicity, the total iron content, as well as the reductive substance content. The solid PFS was conducted structure and morphology measurements such as X-ray diffraction (XRD), Fourier-transform infrared spectroscopy (FT-IR), and scanning electron microscopy (SEM). In addition, the PFS coagulation performance in treating kaolin model suspension was studied as well.

2. Experiment

2.1. Materials

The main properties of ion-exchange membranes (IEM) used in this experiment are listed in Table 1. The chemicals, such as $FeSO_4$, H_2SO_4, and Na_2SO_4, etc., are of analytical pure grades. They were purchased from a chemical reagents company in China. Commercial liquid PFS were provided by Laiwu Hongshen Water Purification Materials Co., Ltd., China. Distilled water was used throughout.

2.2. Experiment set-up

Fig. 1 shows the schematic diagrams of the ED and BMED. The ED stack consists of five repeating units, each

Table 1
Main properties of the ion-exchange membranes used in the experiments

Membrane type	Thickness (μm)	Water content (%)	Transport number (%)	Burst strength (MPa)	Area resistance (Ω/cm²)
AM	0.20	35–40	>98	>0.35	0.5–1.5
CM	0.15	35–40	>98	>0.35	0.5–1.5
BP	0.16–0.23	35–40	/	>0.25	/

Data were referred to Beijing JieRui Environment Protection Technology Co., Ltd., China.

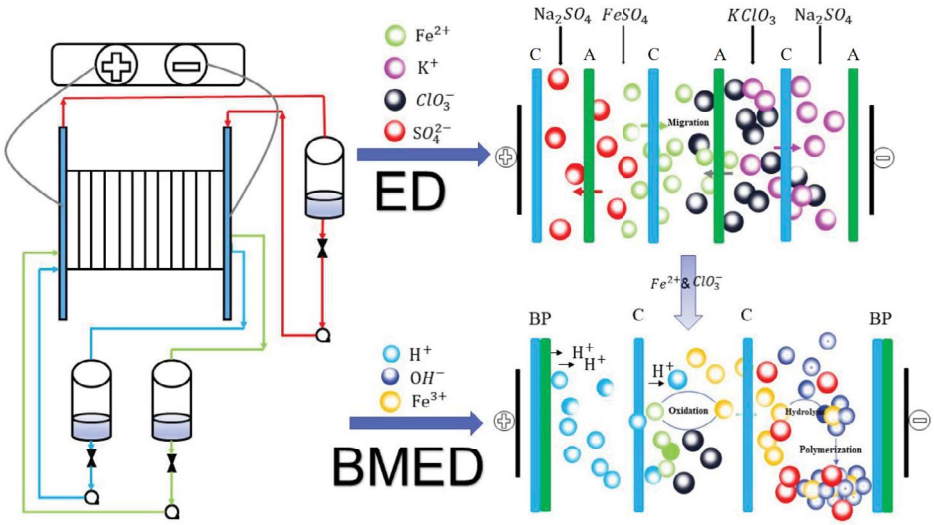

Fig. 1. Schematic diagrams of the electrodialysis and bipolar membrane electrodialysis.

unit equipped with a anion-exchange membrane (A_1) and a cation-exchange membrane (C_1) in series. Each unit is divided into a dilute compartment and a concentrate compartment. The BMED stack is composed of five repeating units, each unit installed with a bipolar membrane (BM) and two cation-exchange membranes (C_1&C_2) in series. Each unit is divided into an acid compartment, a feed compartment, and a base compartment, respectively. Spacers with 0.7 mm are used to isolate each membrane. Each membrane has an effective surface area of 189 cm².

The ED experimental setup consists of four tanks for the electrode solution, $FeSO_4$ solution, $KClO_3$ solution and concentrated solution, respectively. The BMED experimental setup is composed of four tanks for the electrode solution, feed solution, acid solution and base solution, respectively. The tanks are connected to the membrane stack compartments by submersible pumps, respectively. The electrode tank is filled with 1 L 3% Na_2SO_4 solution. The dilute tank and feed tank are filled with 1 L raw solution, and the other tanks contain 1 L deionized water.

The membrane stack is attached to a regulated current-voltage/current-current (CV/CC) power supply (QJ3005, from Ningbo Jiuyuan Electrical Instrument Ltd., China) through the graphite (cathode) and titanium coated with ruthenium (anode). Before the supply of current/voltage drop, the solution of each tank should be circulated for 10 min to eliminate the gas bubbles which trapped on the surface of membranes [17].

2.3. Analytical methods

2.3.1. Calculation of current efficiency and energy consumption during ED process

Current efficiency and energy consumption are very important for evaluating the electrodialysis process.

The current efficiency in the process is calculated with Fe^{2+} in the concentration compartment with Eq. (1) [18] (Experimental data shows that only a small amount of Fe^{3+} is generated during the ED process, so it is ignored).

$$\eta = \frac{-\left(C_t - C_0\right)V_t F}{NIt} \times 100\% \tag{1}$$

where C_t and C_0 are the concentration of Fe^{2+} in the concentration compartment at time t and time 0, respectively. Z represents the absolute valence of Fe^{2+}, V_t represents the circulating volume of the feed liquid in the concentrated compartment at time t (Note: During the experiment, the volume changes with time), F is the Faraday constant (F = 96,485 c/mol), I is the current, and N is the number of repeating units (N = 5).

The energy consumption E (kW·h/kg) was obtained as Eq. (2) [19]:

$$E = \int_0^t \frac{U_t I d_t}{C_t V_t M} \tag{2}$$

where C_t (mol/L) and V_t (L) represent the Fe^{2+} concentration and the solution volume at time t in the concentration compartment, respectively; U_t (V) refers to the applied voltage drop at time t (h); M is the molar weight of Fe^{2+} (56 g/mol).

2.3.2. Characterizations of liquid PFS

The pH (1%, sol.) was acquired by detecting the pH of the diluted PFS solution (1%, sol.) using the pH meter (FE20, Mettler Toledo Instruments (Shanghai) Co., China.). PFS density was obtained by the weighing 1 mL liquid PFS using electronic balance (YP502N, Jingmi Instruments (Shanghai) Co., China). Conductivity was acquired by conductivity meter (DDS307 Leici Instruments (Shanghai) Co., China.)

The total iron content was measured according to Chinese National Standards (GB 14591-2016). $TiCl_3$ solutions were used to reduce all the Fe^{3+} in samples, and standard $K_2Cr_2O_7$ solution was used to titrate samples with diphenylamine sodium sulfonate as an indicator. The total iron content can be calculated as follows (GB 14591-2016).

$$X_1 = \frac{VC_{K_2Cr_2O_7} \cdot 0.05585}{m} \times 100\% \quad (3)$$

where X_1 is the total iron concentration (wt.%), V is the consumed $K_2Cr_2O_7$ solution volume (mL), $CK_2Cr_2O_7$ is the standard $K_2Cr_2O_7$ solution concentration (mol/L), m is the liquid PFS sample mass (g), and 0.05585 is the 0.001 mol·Fe·mass (g/mol).

The reductive substance content was also determined according to Chinese National Standards (GB 14591-2016). H_3PO_4 buffered solution was used to provide an acidic solution environment for samples, and then standard $KMnO_4$ solution was used to titrate samples. The calculation formula of reductive substance content is shown in Eq. (4).

$$X_2 = \frac{(V - V_0)C_{KMnO_4} \cdot 0.05585}{m} \times 100\% \quad (4)$$

where X_2 is the reductive substance content (wt.%), V is the consumed $KMnO_4$ solution volume (mL), V_0 is the consumed $KMnO_4$ solution volume (mL) of distilled water blank test, $KMnO_4$ is the standard $KMnO_4$ solution concentration (mol/L), 0.05585 is the 0.001 mol·Fe·mass (g/mol), and m is the liquid PFS sample mass (g).

Basicity was measured according to Chinese National Standards (GB 14591-2016). KF solution was introduced to cover the iron ions in samples, which were then titrated with standard NaOH solution with phenolphthalein as an indicator. The basicity is calculated as:

$$B = \frac{\left[(V_0 - V)C_{NaOH} \cdot 0.0170\right]/17.0}{mX_2/18.62} \times 100\% \quad (5)$$

where B is the basicity (wt.%), V is the consumed NaOH solution volume (mL), V_0 is the consumed NaOH solution volume (mL) of distilled water blank test, C_{NaOH} is the standard NaOH solution concentration (mol/L), m is the liquid PFS sample mass (g), X_2 is the reductive substance content (wt.%), 0.017 is the mass (g) of 0.001 mol·OH^-, 17.0 is the mass (g) of 1 mol·OH^-, 18.62 is the 1/3 mol·Fe·mass (g/mol).

2.3.2. Characterizations of solid PFS

In this section, the main research target is solid PFS, which was obtained by freeze-drying the liquid products for over 36 h using a freezer dryer (LGJ-10C, Four-Ring Science Instrument Plant Beijing Co., Ltd., China.). Then, the solid PFS was ground using a mortar and pestle for further analysis, such as SEM, XRD, and FT-IR. The morphology of the solid PFS was detected by SEM using field emission scanning electron microscope (JSM 840, JEOL. Co.). The crystalline phase of the solid PFS was measured by X-ray diffractometer with Cu Kα radiation in the range of 5°–60° (2θ), at a scan rate of 0.02°/s. (1710 APD, Philips, Co., The Netherlands). FT-IR spectroscopy was recorded with a Spectrophotometer (EQUINOX-55, Bruker, Co.) and the spectra were recorded in the range of 4,000–400 cm^{-1}. In which 1 mg solid PFS was mixed with 250 mg·KBr powder to prepare a pellet.

2.3.2.1. Coagulation experiments

According to the relevant literatures, the coagulation experiments were conducted with Kaolin model suspension [20–23]. After adding the coagulants, 250 mL suspension (83 NTU, 0.1 g/L) was stirred rapidly at 250 rpm for 2 min, and then at 50 rpm for 4 min. Finally, the suspension was left to settle for 20 min, and samples were collected at 2 cm below the solution surface to determine the turbidity.

Turbidity was measured through determining the sample absorbance by ultraviolet spectrophotometer (VIS-7220G, Beijing Beifen–Ruili analytical instrument (Group) Co., Ltd., China), and the standard equation is shown in Eq. (6).

$$A = 338.8T\left(R^2 = 0.9997\right) \quad (6)$$

where A is the suspension absorbance and T is the suspension turbidity. The turbidity removal ratio (R) was calculated by Eq. (7):

$$R = \frac{T_0 - T_t}{T_0} \times 100\% \quad (7)$$

where T_0 (NTU) is the initial suspension turbidity before coagulation experiments, T_t (NTU) is the suspension turbidity at time t after the coagulation runs.

2.4. Energy consumption during BMED process

Generally, the total energy consumption was calculated based on target product generated by a bipolar membrane. But it is difficult to determine the amount of OH^- in reaction tank because of the formation of inorganic polymer. As we know, the amount of H^+ generated by bipolar membrane is equal to that of OH^-, theoretically. Therefore, in this passage, the total energy consumption E (kW·h/(kg H_2SO_4)) was calculated based on the amount of H^+ in acid tank, and as shown in Eq. (8).

$$E = \int_0^t \frac{U_t I dt}{(C_t - C_0)VM} \quad (8)$$

where U_t (V) is the voltage drop across the membrane stack at time t, I (A) is the current, C_0 and C_t (mol/L) are the H_2SO_4 concentrations at time 0 and t in acid tank, V (L) is the acid tank volume, and M (g/mol) is H_2SO_4 molar molecular weight. The acid concentration was determined by titrating with a standard NaOH solution with phenolphthalein as an indicator.

3. Results and discussion

3.1. Concentrating raw solution through ED process

3.1.1. Effect of current density on ED process

Electrodialysis (ED) is a method to concentrate and purify the solution by using the selective permeability of ion-exchange membrane to ions in the solution under the action of electric field. In this section, the solution of high concentration of Fe^{2+} and ClO_3^- was prepared by ED stack as shown in Fig. 2 and the solution will be used as raw material for PFS preparation.

The experiment was conducted at room temperature. In the following experiments, the feed concentration was 4.2 mol/L $FeSO_4$ and 0.7 mol/L $NaClO_3$, respectively, and the flow rate was set to 0.1 mL/min, different current densities (10, 20 and 30 mA/cm^2) and operating time were selected to investigate the ED concentration process of raw solution which main contains Fe^{2+} and ClO_3^-. For the reliability of the experimental data, three parallel experiments were carried out for each experiment.

Fig. 2a shows the effect of current density on the stack voltage drop as the operating time increases. It can be seen from Fig. 2a that the changing trend of the voltage drop with time is almost the same, and they all show a "U" shape that decreases first, then stabilizes, and finally increases. This is because in the initial stage, ions migrate under the action of electric field force, resulting in an increase of ions

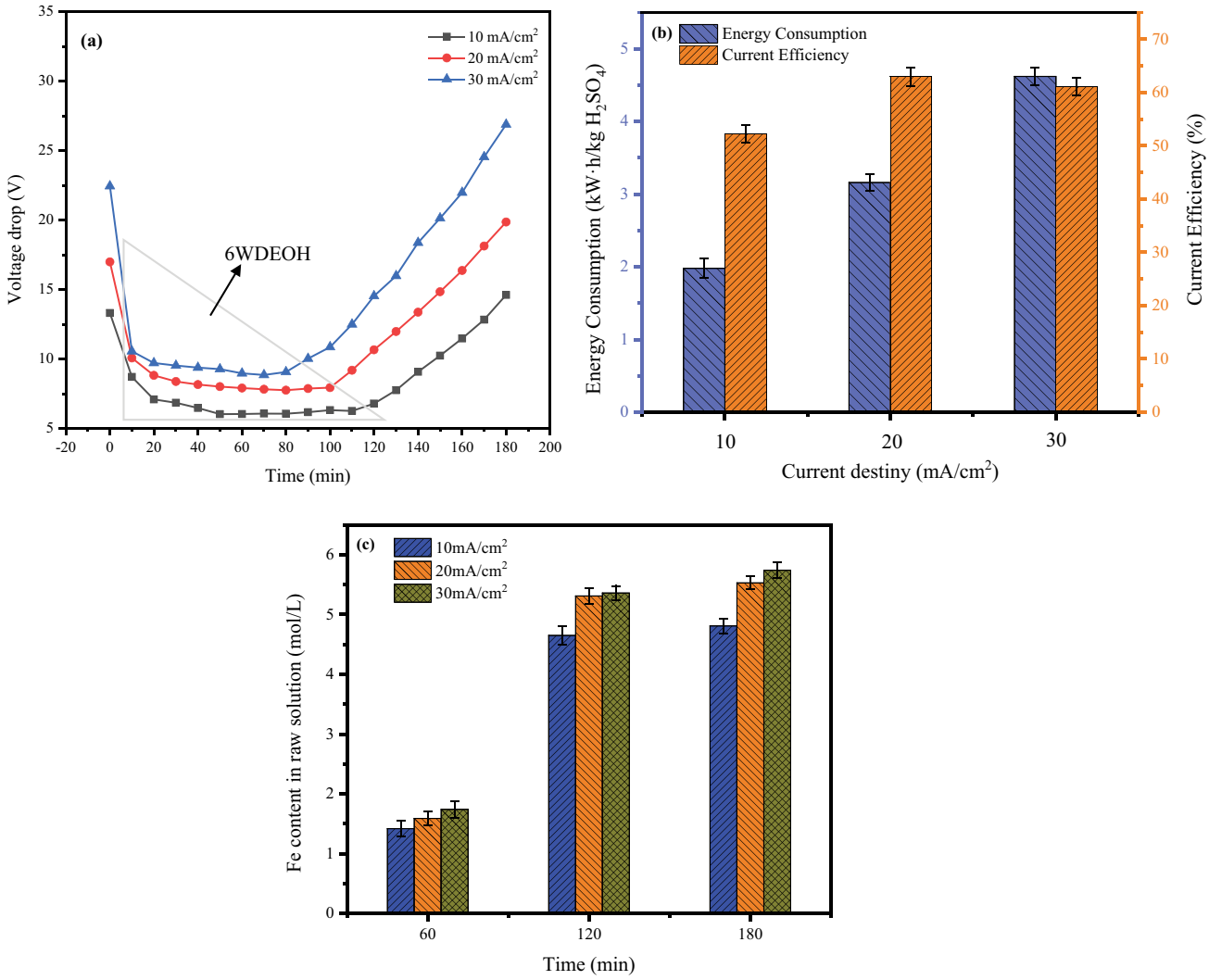

Fig. 2. Effect of current density on voltage drop (a), current efficiency and energy consumption (b), total iron content in raw solution (c) during electrodialysis process.

concentration in the concentration compartment and a decrease of the membrane stack resistance. As the process progresses, electrodialysis maintains a relatively stable state in the medium term. Afterward, due to the decrease of the ion concentration in the dilution compartment, the membrane stack resistance increases rapidly, which caused the voltage drop of the membrane stack increase significantly. In addition, Fig. 2a also shows that the voltage drop of the membrane stack increases with the increase of current density.

Fig. 2b shows the effect of current density during ED process on current efficiency, energy consumption, and total iron content in the raw solution. As can be seen from Fig. 2b, when the current density is 20 mA/cm^2, the current efficiency reaches the maximum value, which is 62.92%. When the current density increases to 30 mA/cm^2, the current efficiency is lower than 20 mA/cm^2. This is because with the increase of current density, part of the water splits on the surface of the membrane into H^+ and OH^-. The hydration radius of the H^+ and OH^- are smaller than Fe^{2+}, which easily penetrates the membrane and reduces the transfer efficiency of Fe^{2+}. Meanwhile, the high current density leads to increased water penetration, further reducing the current efficiency. In the previous literature, the study found that the increase in current density will lead to an increase in energy consumption, because most of the electrical energy is consumed in the membrane stack resistance, the experimental results also confirmed this fact. Fig. 2c shows the effect of current density on the quality of the raw solution obtained in the ED process. The Fe^{2+} content in the raw solution is mainly used as the judgment criterion because the Fe^{2+} content will directly affect the performance of the prepared flocculant in the following experiment. It can be seen from Fig. 2c that as the current density increases, the iron content in the resulting raw solution also increases. When the current density is 30 mA/cm^2, the iron content reaches a maximum of 5.74 mol/L in 120 min. However, it is worth noting that the current density is 20 mA/cm^2, and the Fe^{2+} content is not much different from 30 mA/cm^2 when running for 120 min.

3.1.2. Effect of feed concentration on ED process

In this part of the experiment was carried out under the conditions of room temperature and current density of 20 mA/cm^2, and the influence of the feed concentration was investigated. The feed concentration of $FeSO_4$ are 4.8, 4.2, and 3.6 mol/L, the concentration of $NaClO_3$ are 0.8, 0.7, and 0.6 mol/L, correspondingly.

Fig. 3a shows the effect of feed concentration on the voltage drop as the operating time increases. It can be seen from Fig. 3a that the change trend of the voltage drop with time is almost the same, and they all show a "U" shape that decreases first, then stabilizes, and finally increases. The greater the concentration of the feed solution, the lower the voltage drop in the stable phase. This is because the concentration of ions in the solution is large, the resistance of the membrane stack is small during operation, and the voltage drop will decrease when the applied current is constant.

Fig. 3b shows the effect of feed concentration on the current efficiency and energy consumption of the electrodialysis process. For the current efficiency, it can be seen from the experimental results that the current efficiency reaches the maximum when the concentration is 4.2 mol/L, and when the concentration continues to increase, the current efficiency will decrease from 64.51% to 63.07%, which is due to the excessive solution concentration A large concentration difference is formed between the feed chamber and the concentration chamber, which leads to the permeation of water molecules between the two chambers through the ion-exchange membrane, which hinders the migration of Fe^{2+} to a certain extent. The increase in feed concentration also causes an increase in energy consumption in the ED process. And when the concentration increases from 4.2 to 4.8 mol/L, the increase in energy consumption is much larger than when the concentration increases from 3.6 to 4.2 mol/L. This is because the greater the initial concentration, the more Fe^{2+} accumulates on the surface of the membrane, causing membrane fouling, hindering ion migration, increasing energy consumption, and reducing current efficiency.

Fig. 3c shows the influence of the feed concentration on the Fe^{2+} concentration in the raw solution obtained in the concentration chamber. The greater the feed concentration and the longer the operation time, the greater the Fe^{2+} concentration in the final raw solution. When the feed concentration is 4.2 and 4.8 mol/L, the operating time is about 60–120 min, and Fe^{2+} concentration increases the fastest, which is consistent with the voltage drop in Fig. 3a. The voltage drop is in a stable state. When the operating time continues to extend, the Fe^{2+} concentration increases less. It is because the increase of the ion concentration in the concentration chamber forms a certain resistance to ion migration, and during the experiment, some ions gather on the surface of the ion-exchange membrane, which reduces the particle migration performance of the ion-exchange membrane. Similarly, the greater the initial concentration, the more serious the accumulation on the membrane surface, so the operation time is 120–180 min, the increase of Fe^{2+} concentration in the concentration chamber is not obvious, but it will affect the energy consumption of the operation process. This also explains the large increase in energy consumption in Fig. 3b.

Taking into account that the higher the current density, the higher the energy consumption, and the excessive initial concentration will cause membrane fouling and higher energy consumption, and the increase in Fe^{2+} concentration in the raw solution will not be significantly increase when the operating time is 120–180 min, so the subsequent experiment uses a current density of 20 mA/cm^2 and runs for 120 min to prepare a raw solution for subsequent experiments.

3.2. Preparing liquid PFS through BMED process

The process of oxidation, hydrolysis and polymerization in the preparation of PFS can be precisely controlled by adjusting the operation parameters of the electrodialysis process. In this part, we use the H^+ generated by bipolar membrane electrodialysis to acidify the raw solution prepared in the ED process, thereby promoting the oxidation process of ferrous ions. Under the action of the electric field, the Fe^{3+} migrate to the alkali compartment, and polymerizes with the OH^- produced by hydrolysis on the bipolar exchange

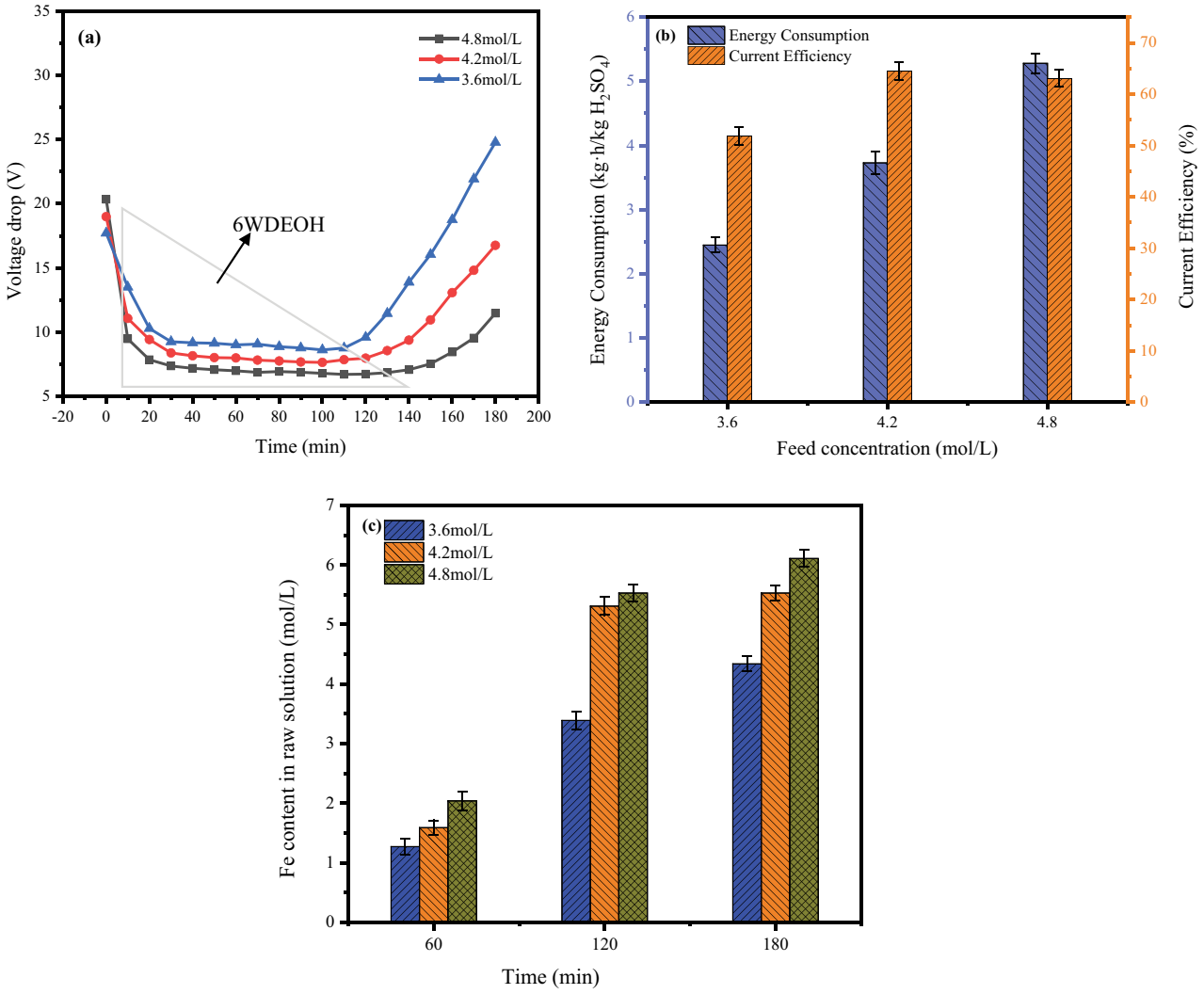

Fig. 3. Effect of feed concentration on voltage drop (a), current efficiency, energy consumption (b), total iron content in raw solution (c) during electrodialysis process.

membrane to produce liquid PFS. This part mainly investigates the influence of current density, feed flow rate and sulfuric acid addition on voltage drop, pH in acid compartment, energy consumption and liquid PFS performance. All experiments were conducted at room temperature.

3.2.1. *Effect of current density*

The specific operating conditions for this part are as follows: take 1 L of raw solution prepared in step 1 as the salt chamber feed solution, add an equal volume of 0.1 mol/L H_2SO_4 to the acid chamber, and add an equal volume of deionized water to the alkali chamber. The current densities are 10, 20 and 30 mA/cm^2. The feed flow rate is set to 0.1 L/min.

Like electrodialysis, most of the electrical energy in bipolar membrane electrodialysis is also used to overcome the resistance of the membrane stack. It can be seen from Fig. 4a that regardless of the initial voltage in the initial stage, the voltage drop will be slightly reduced, and then it will remain relatively stable for the next period, and there will be an upward trend in the later period. This is because most of the ions in the solution form a flocculant, which causes the concentration of ions in the solution to drop, the voltage of the membrane stack gradually increases, and the pressure drop also tends to increase. Fig. 4b shows the effect of current density on the pH in the acid chamber, further illustrating the bipolar membrane's ability to split water. The higher the current density, the more H^+ produced by the hydrolysis dissociation of the bipolar membrane, resulting in a lower pH in the acid chamber. At the same time, the current density has a certain influence on the selective permeability of the membrane, so the pH is not strictly proportional to the operating time. Between the operating time of 40–120 min, the generation rate and migration rate are almost the same, the accumulation of hydrogen ions in the acid chamber is less, and the pH change is not obvious. As the experiment progresses, Fe^{2+} in the salt chamber is exhausted and H^+ accumulate in the salt chamber, which hinders the migration of hydrogen ions in the acid chamber to a certain extent. The

H^+ in the acid chamber continue to accumulate and the pH decreases. Fig. 4b also shows the change of solution conductivity with current density, and the conductivity of the salt chamber shows a downward trend. This is because under the action of an external electric field, Fe^{2+} in the salt chamber is continuously oxidized to Fe^{3+}, and then migrates out of the salt chamber into the alkali chamber, resulting in a continuous decrease in the number of charged ions in the salt chamber and a decrease in conductivity. The Fe^{3+} combines with the OH^- produced by the bipolar membrane electrolyzed water to form a polymer, which further reduces the ion concentration. It can also be seen from the figure that the greater the current density, the faster the conductivity drops. This is because the greater the current density, the greater the ion migration rate, and the faster the conductivity drops.

Fig. 5 shows the energy consumption changes in the BMED process and turbidity removal rate of liquid PFS. As the current density increases from 10 to 30 mA/cm², the energy consumption decreases from 2.93 to 1.52 kW·h/kg H_2SO_4. This seems to be related to Eq. (6) The greater the current density is, the higher the energy consumption is. On the contrary, after consulting relevant literature and analyzing the experimental results, we believe that this is due to the increase in the current density, which increases the reaction rate, accelerates the production rate of the product, and shortens the reaction time. reduce. According to GB14591-2016, the liquid PFS obtained under different current densities is analyzed, and the main data is shown in Table 2. The increase in current density from 10 to 20 mA/cm² contributes to the generation of PFS. It can also be seen from the results of the flocculation experiment that the flocculant obtained with a current density of 20 mA/cm² has the best flocculation effect, as shown in Fig. 5.

3.2.2. Effect of feed flow rate

Based on the effect of current density experiment, the influence of the feed flow rate is further explored. The experiment was carried out at room temperature. During the

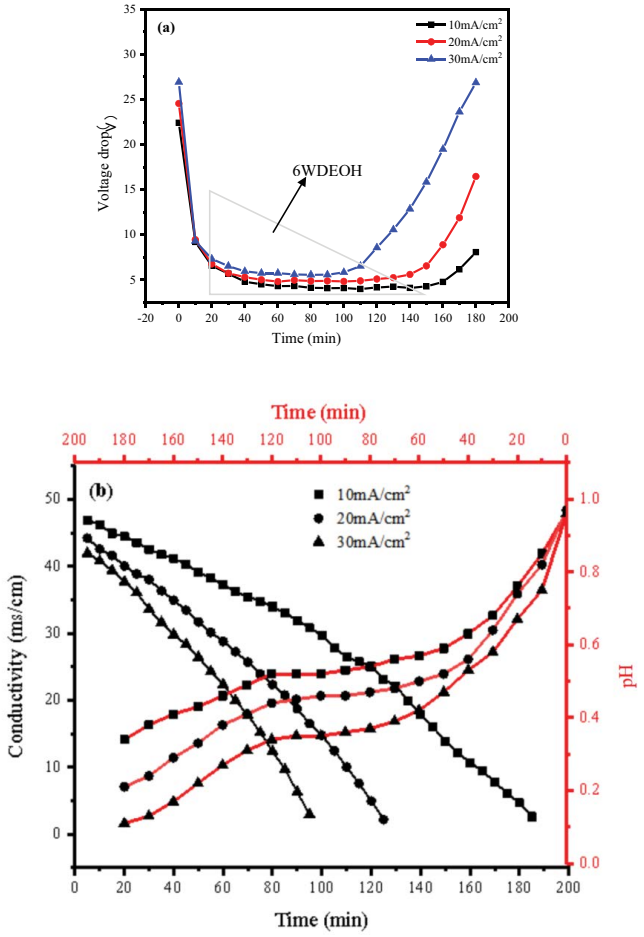

Fig. 4. Effect of current density on voltage drop (a), pH in acid chamber (b), and conductivity of the solution (c) during bipolar membrane electrodialysis process.

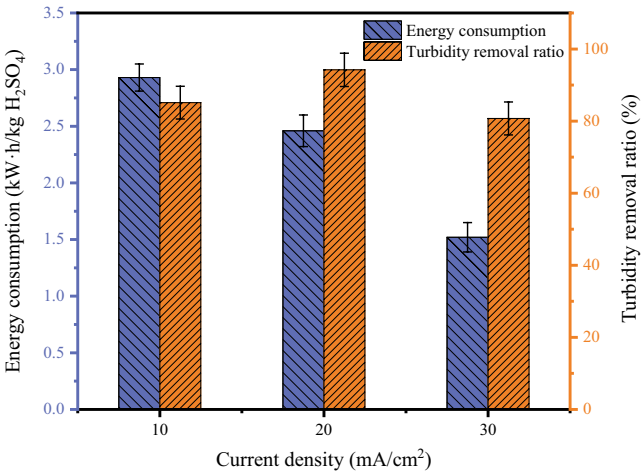

Fig. 5. Effect of current density on energy consumption in the bipolar membrane electrodialysis process and turbidity removal rate of liquid PFS.

Table 2
Effect of current density on product quality

Current density (mA/cm²)	10 mA/cm²	20 mA/cm²	30 mA/cm²
pH (1%, sol)	2.78	2.42	2.08
Density (g/cm³)	1.48	1.68	1.57
Basicity (%)	11.73	16.85	21.04
Total iron content (%)	12.23	13.47	11.02
Reductive substance content (Fe^{2+}; %)	0.0061	0.0048	0.0057

experiment, the current density was maintained at 20 mA/cm^2, and the feed rate was 0.10, 0.20, and 0.30 L/min. Take 1 L raw solution as the feed solution of the salt chamber, add an equal volume of 0.1 mol/L dilute sulfuric acid solution to the acid chamber, and add an equal volume of deionized water to the alkali chamber.

Different feed flow rates will also affect the performance of the BMED, thereby affecting the performance of the resulting liquid PFS. In this experiment, the changes in voltage drop, conductivity, and pH in the acid chamber were explored by adjusting different feed flow rates. As shown in Fig. 6a, with the increase of the feed tassels, the voltage drop rapidly decreases. This is because a larger feed flow rate can quickly supplement the ion concentration in the membrane stack and reduce the membrane stack voltage. As the particles migrate and react in the membrane stack, the ion concentration of the entire system decreases, which leads to an increase in the voltage of the membrane stack. This change is in line with the voltage change trend of bipolar membrane electrodialysis.

Fig. 6b investigates the effect of feed flow rate on conductivity and pH in the acid chamber. The greater the flow rate, the faster the change in conductivity and the greater the change in ion concentration. As for the pH change in the acid chamber, firstly, because the current applied to the membrane stack remains stable, the change of the feed flow rate is basically the same. At the same time, it can be seen from the figure that the change of pH is smaller at a larger feed flow rate. This is because the current applied to the membrane stack is mainly used for ion migration rather than water electrolysis.

At the same time, experiments and calculations were performed on the energy consumption and turbidity removal rate under different feed flow rates. It can be seen from Fig. 7 that as the feed flow rate increases, the energy consumption gradually decreases, which is due to the faster feed rate. The material flow rate accelerates the ion migration rate and promotes the reaction, but the turbidity removal rate of the product does not change much, indicating that the feed flow rate has little effect on the quality of the product.

3.2.3. Effect of sulfuric acid addition

Based on the above experiment, we explored the influence of the sulfuric acid addition is further. The experiment was carried out at room temperature. During the experiment, the current density was maintained at 20 mA/cm^2, and the feed rate was 0.10, 0.20, and 0.30 L/min. Take 1 L raw solution as the feed solution of the salt chamber, add an equal volume of 0.1 mol/L dilute sulfuric acid solution to the acid chamber, and add an equal volume of deionized water to the alkali chamber.

Fig. 8a shows the change in the voltage drop of the membrane stack when the amount of sulfuric acid added in the acid chamber changes. When the amount of acid added is high, a large amount of hydrogen ions migrates through the membrane stack to the salt chamber and react with Fe^{2+} to form Fe^{3+}. The ion current formed during the migration reduces the voltage of the membrane stack. Therefore, the more acid is added, the lower the voltage of the membrane stack. The faster the reaction rate, the faster the Fe^{3+} consumption, and the shorter the stable operation time. Fig. 8b shows the effect of different sulfuric acid additions in the acid chamber on the conductivity and pH of the acid

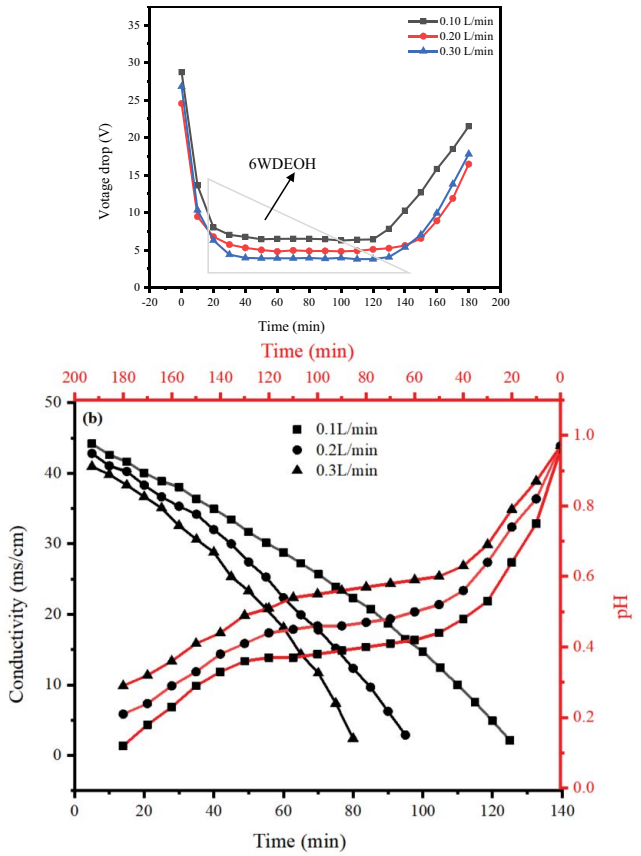

Fig. 6. Effect of feed flow rate on voltage drop (a), pH in acid chamber and conductivity of the solution (b) during bipolar membrane electrodialysis process.

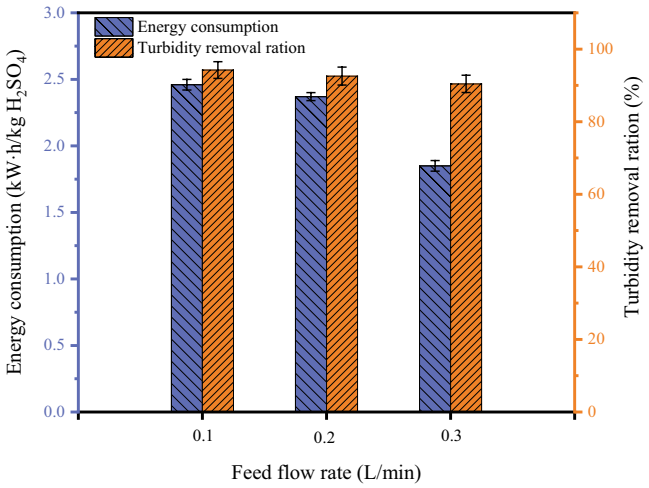

Fig. 7. Effect of feed flow rate on energy consumption in the bipolar membrane electrodialysis process and turbidity removal rate of liquid PFS.

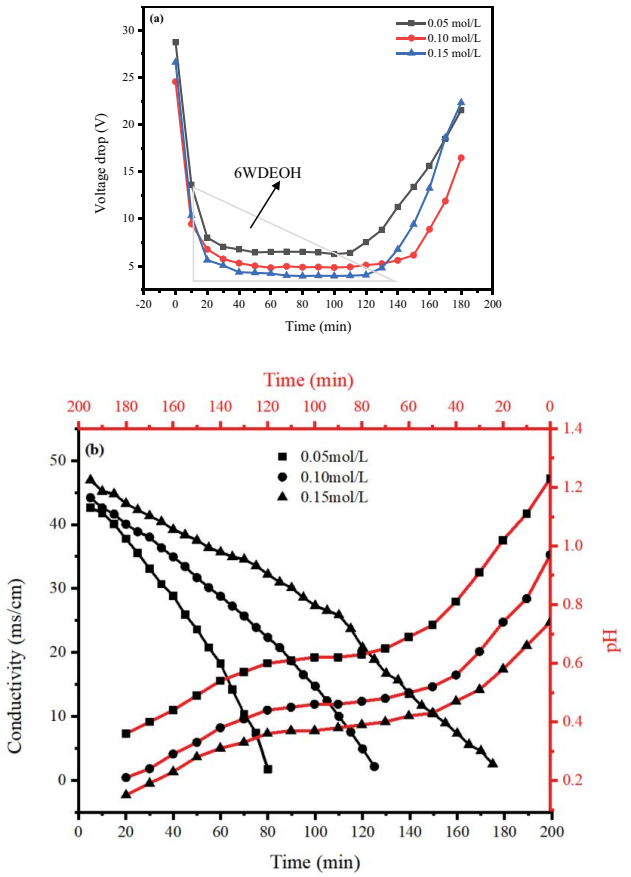

Fig. 8. Effect of sulfuric acid addition on voltage drop (a), pH in acid chamber, and conductivity of the solution (b) during bipolar membrane electrodialysis process.

chamber. When the initial acid addition is large, the number of charged ions is large, and the conductivity is large. Under the same current, the migration rate is constant, so the conductivity decreases slowly. As for the pH in the acid chamber, due to the constant current and the ion migration rate within a certain range, the overall downward trend is basically the same. However, when the amount of sulfuric acid in the acid chamber is large, a large amount of hydrogen ions migrates to the salt chamber. The reaction causes more unmigrated Fe^{3+} to be retained in the salt chamber, which adheres to the surface of the cation exchange membrane and causes a certain steric hindrance, thereby reducing the migration rate of hydrogen ions. Therefore, the three curves are not completely parallel.

Regarding the energy consumption of the BMED process, it is found through experiments that as the addition of sulfuric acid in the acid chamber increases, the energy consumption of the process can be reduced. This is due to the large ion concentration, the small resistance of the membrane stack, and the small voltage drop. According to the energy consumption calculation formula. The energy consumption decreases with a certain current density. This is consistent with the voltage drop trend in Fig. 8a. Fig. 9 shows that the increase in the addition of sulfuric acid leads to a change in the turbidity removal rate, which generally

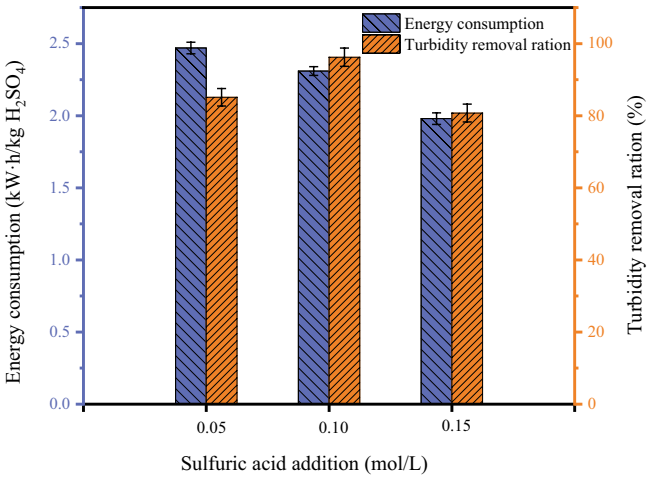

Fig. 9. Effect of sulfuric acid addition on energy consumption in the bipolar membrane electrodialysis process and turbidity removal rate of liquid PFS.

shows a trend of first increasing and then decreasing. It is speculated that this phenomenon is mainly caused by the migration of hydrogen ions. When the addition of sulfuric acid is less than 0.10 mol/L, hydrogen ions migrate to the salt chamber to react with Fe^{2+}, but when the sulfuric acid addition continues to increase, the hydrogen ions that are too late to participate in the reaction in the salt chamber will migrate to the alkali chamber to neutralize the alkali The hydroxide ions in the chamber cause the decrease of the flocculation ability of the liquid PFS.

3.2.4. Characterizations of solid PFS

A freeze dryer was used to dry the liquid PFS product, and the morphology and main functional groups of the obtained solid PFS were characterized by SEM and FT-IR and compared with commercial PFS. The reason for the good flocculation effect was explored from the structure of PFS.

As shown in Fig. 10, the micrographs of the samples in this study are similar to those of commercial PFS. Similarly, the PFS sample appears as an amorphous material, forming many aggregates of various sizes and shapes.

It can be seen from Fig. 11 that the crystallinity of the solid sample is fuzzy and amorphous, which is consistent with the SEM result. According to those reported in the literature [12]. The shoulder at 10°–30° 2θ, which can be ascribed to iron-based compounds.

Fig. 12 illustrates the FT-IR spectra of PFS samples. Generally speaking, the five spectra are quite similar. First, the characteristics bond at the 3,250–3,000 cm^{-1} can be attributed to the stretching vibration of –OH, while that at the about 1,628 cm^{-1} can be attributed to the stretching vibration of water absorbed or complexed. The peaks in the region of 1,160–1,120 cm^{-1} can be assigned to the symmetric stretch of the S=O and/or the O=S=O bonds. In addition, there exhibits a characteristic peak at 1,000–980 cm^{-1} which is assigned to the bending vibration band of Fe–OH. A considerably weaker band in the region 680–610 cm^{-1} can be attributed to the $SO4^{2-}$ [13].

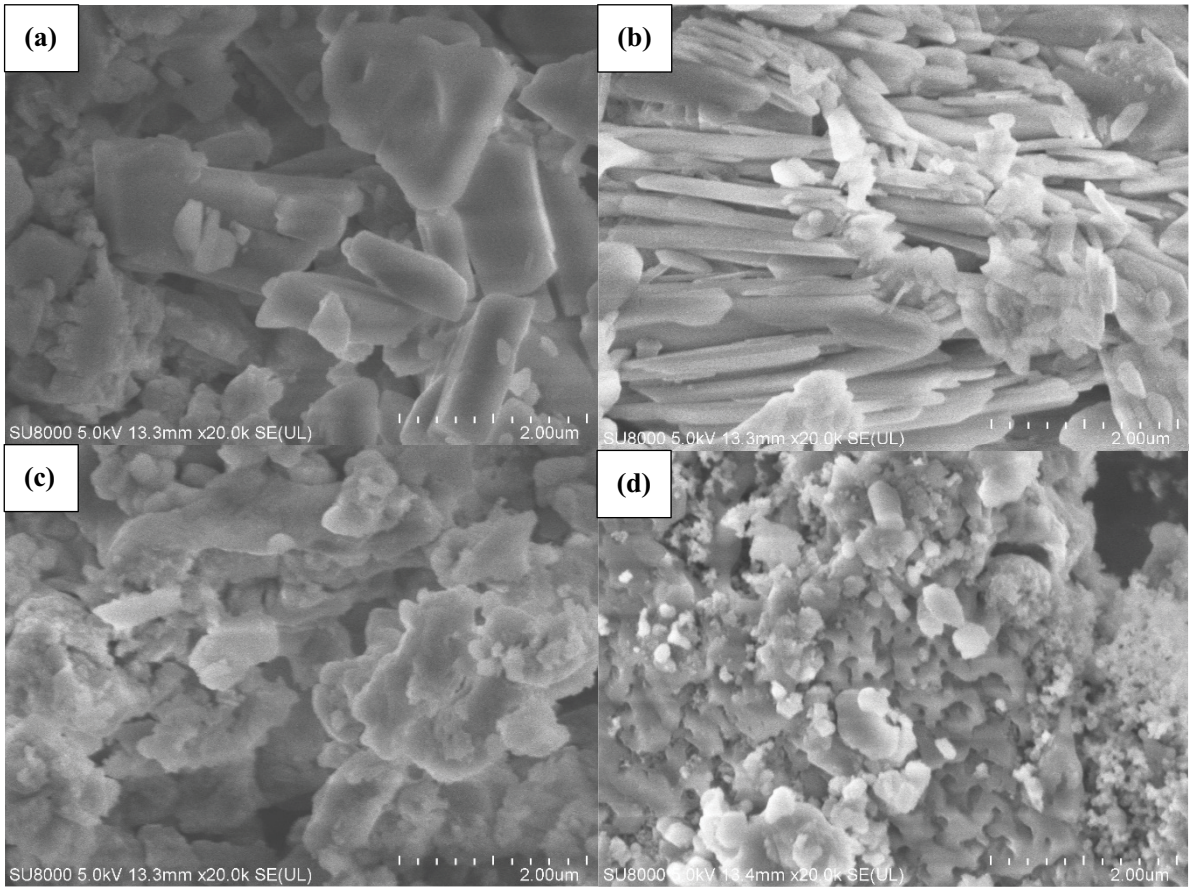

Fig. 10. Scanning electron microphotographs of PFS samples. (a) Commercial PFS. (b) i = 10 mA/cm², feed flow rate = 0.1 L/min, sulfuric acid addition = 0.1 mol/L. (c) i = 20 mA/cm², feed flow rate = 0.2 L/min, sulfuric acid addition = 0.1 mol/L. (d) i = 20 mA/cm², feed flow rate = 0.1 L/min, sulfuric acid addition = 0.15 mol/L.

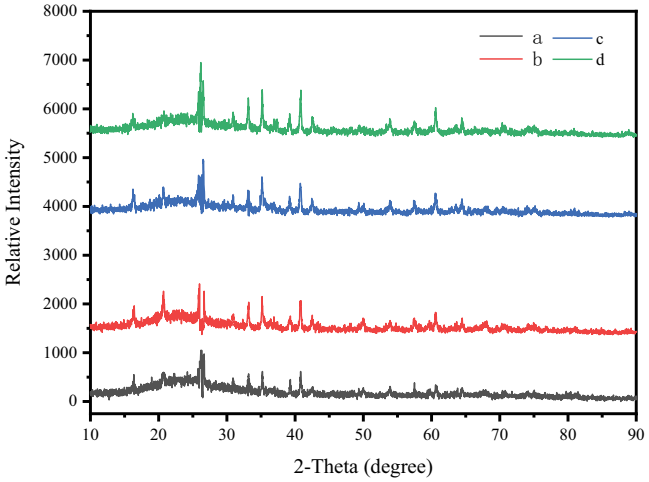

Fig. 11. X-ray diffraction patterns of PFS samples. (a) Commercial PFS. (b) i = 10 mA/cm², feed flow rate = 0.1 L/min, sulfuric acid addition = 0.1 mol/L. (c) i = 20 mA/cm², feed flow rate = 0.2 L/min, sulfuric acid addition = 0.1 mol/L. (d) i = 20 mA/cm², feed flow rate = 0.1 L/min, sulfuric acid addition = 0.15 mol/L.

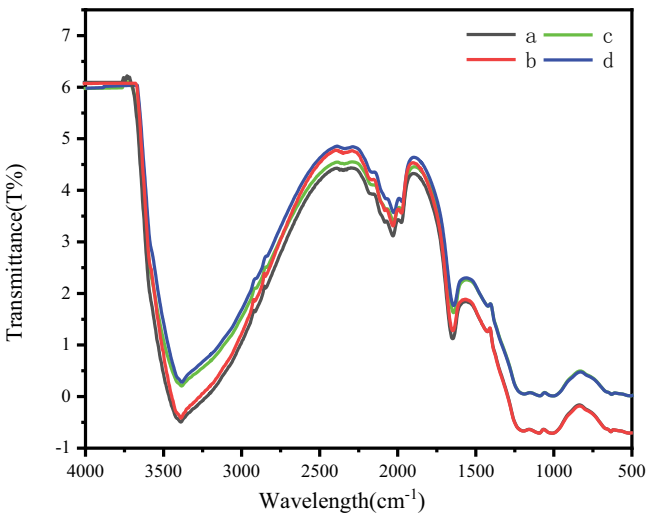

Fig. 12. Fourier-transform infrared spectroscopy of PFS samples. (a) Commercial PFS. (b) i = 10 mA/cm², feed flow rate = 0.1 L/min, sulfuric acid addition = 0.1 mol/L. (c) i = 20 mA/cm², feed flow rate = 0.2 L/min, sulfuric acid addition = 0.1 mol/L. (d) i = 20 mA/cm², feed flow rate = 0.1 L/min, sulfuric acid addition = 0.15 mol/L.

Table 3
Effect of feed flow rate on product quality

Feed flow rate (L/min)	0.1	0.2	0.3
pH (1%, sol)	2.78	2.72	2.81
Density (g/cm^3)	1.48	1.56	1.63
Basicity (%)	11.73	15.57	19.36
Total iron content (%)	12.23	12.74	12.53
Reductive substance content (Fe^{2+}; %)	0.0061	0.0058	0.0059

Table 4
Effect of sulfuric acid addition on product quality

Sulfuric acid addition (mol/L)	0.05	0.10	0.15
pH (1%, sol)	2.86	2.42	2.13
Density (g/cm^3)	1.48	1.68	1.45
Basicity (%)	10.25	14.85	11.42
Total iron content (%)	13.37	13.47	14.21
Reductive substance content (Fe^{2+}; %)	0.0073	0.0048	0.0039

4. Conclusions

The experiment explored the combination of electrodialysis and bipolar membrane electrodialysis to prepare poly-ferric sulfate flocculant. The effects of some experimental parameters such as current density, feed flow rate and sulfuric acid addition on the quality of the flocculant were investigated. When the current density is 30 mA/cm^2, the alkalinity reaches 21.04% and the energy consumption is 1.52 kW·h (kg H_2SO_4), the turbidity removal rate reaches a maximum of 94.23% when the current density is 20 mA/cm^2, and the energy consumption is 2.46 kW·h (kg H_2SO_4).

After SEM, XRD and FT-IR analysis, the resulting PFS samples are amorphous with rather obscure traces of crystallinity.

References

[1] M.H. Fan, S.W. Sung, R.C. Brown, T.D. Wheelock, F.C. Laabs, Synthesis, characterization, and coagulation of polymeric ferric sulfate, J. Environ. Eng., 128 (2002) 483–490.

[2] J.K. Edzwald, J.E. Tobiason, Enhanced coagulation: US requirements and a broader view, Water Sci. Technol., 40 (1999) 63–70.

[3] Y. Tang, Study on Preparation of Polyciliate Aluminum Ferric Chloride Flocculant From Fly Ash, Qiqihar University, China, 2012.

[4] P.-c. Ke, Z.-h. Liu, L. Li, Synthesis, characterization, and property test of crystalline poly-ferric sulfate adsorbent used in treatment of contaminated water with a high As(III) content, Int. J. Miner. Metall. Mater., 251 (2018) 1217–1225.

[5] P.Y. Liu, Study on the coagulation of poly-ferric sulfate to eliminate organic chlorine in water, China Environ. Sci., 35 (2015) 2382–2392.

[6] M. Liu, P.F. Zhu, Y. Ran, Y.J. Chen, L. Zhou, Preparation, characterization and coagulation performance of a composite coagulant formed by the combination of poly-ferric sulfate (PFS) and Ce^{3+}, Desal. Water Treat., 57 (2015) 13600–13607.

[7] W. Schneider, Hydrolysis of iron(III)…chaotic olation versus nucleation, Comments Inorg. Chem., 3 (1984) 205–223.

[8] H.F. Ma, Study on the Preparation and Optimization Process of Poly-Ferric Sulfate, Tianjin University of Technology, China, 2013.

[9] Q.-B. Chen, Z.-Y. Ji, J. Liu, Y.-Y. Zhao, S.-Z. Wang, J.-S. Yuan, Development of recovering lithium from brines by selective-electrodialysis: effect of coexisting cations on the migration of lithium, J. Membr. Sci., 548 (2018) 408–420.

[10] D.T. Jia, M.Y. Li, G.Q. Liu, P.H. Wu, J.F. Yang, Y. Li, S. Zhong, W. Xu, Effect of basicity and sodium ions on stability of polymeric ferric sulfate as coagulants, Colloids Surf., A, 512 (2017) 111–117.

[11] Y.X. Wei, Y.M. Wang, X. Zhang, T.W. Xu, Comparative study on the treatment of simulated brominated butyl rubber wastewater by using bipolar membrane electrodialysis (BMED) and conventional electrodialysis (ED), Sep. Purif. Technol., 110 (2013) 164–169.

[12] L. Shi, Y.S. Hu, S.H. Xie, G.X. Wu, Z.H. Hu, X.M. Zhan, Recovery of nutrients and volatile fatty acids from pig manure hydrolysate using two-stage bipolar membrane electrodialysis, Chem. Eng. J., 334 (2018) 134–142.

[13] F. Zhang, C.H. Huang, T.W. Xu, Production of sebacic acid using two-phase bipolar membrane electrodialysis, Ind. Eng. Chem. Res., 48 (2009) 7482–7488.

[14] M.J. Miao, Y.B. Qiu, L. Yao, Q.H. Wu, H.M. Ruan, B. Van der Bruggen, J.N. Shen, Preparation of N,N,N-trimethyl-1-adamantylammonium hydroxide with high purity via bipolar membrane electrodialysis, Sep. Purif. Technol., 205 (2018) 241–250.

[15] C.R. Li, G.F. Wang, H.Y. Feng, T.Y. He, Y.M. Wang, T.W. Xu, Cleaner production of Niacin using bipolar membranes electrodialysis (BMED), Sep. Purif. Technol., 156 (2015) 391–395.

[16] X. Zhang, X.Y. Wang, Q.R. Chen, Y. Lv, X.Z. Han, Y.X. Wei, T.W. Xu, Batch preparation of high basicity poly-ferric sulfate by hydroxide substitution from bipolar membrane electrodialysis, ACS Sustainable Chem. Eng., 5 (2017) 2292–2301.

[17] C.X. Jiang, Y.M. Wang, T.W. Xu, An excellent method to produce morpholine by bipolar membrane electrodialysis, Sep. Purif. Technol., 115 (2013) 100–106.

[18] M. Badruzzaman, J. Oppenheimer, S. Adham, M. Kumar, Innovative beneficial reuse of reverse osmosis concentrate using bipolar membrane electrodialysis and electrochlorination processes, J. Membr. Sci., 326 (2009) 392–399.

[19] A.I. Zouboulis, P.A. Moussas, F. Vasilakou, Polyferric sulphate: preparation, characterisation and application in coagulation experiments, J. Hazard. Mater., 155 (2008) 459–468.

[20] Y. Wei, X. Dong, A. Ding, D. Xie, Characterization and coagulation–flocculation behavior of an inorganic polymer coagulant – poly-ferric-zinc-sulfate, J. Taiwan Inst. Chem. Eng., 58 (2016) 351–356.

[21] L. Li, M. Fan, R.C. Brown, J.A. Koziel, J.H. van Leeuwen, Production of a new wastewater treatment coagulant from fly ash with concomitant flue gas scrubbing, J. Hazard. Mater., 162 (2009) 1430–1437.

[22] P.A. Moussas, A.I. Zouboulis, A new inorganic-organic composite coagulant, consisting of poly-ferric sulfate (PFS) and polyacrylamide (PAA), Water Res., 43 (2009) 3511–3524.

[23] K. Nakamoto, Infrared and Raman Spectra of Inorganic and Coordination Compounds, John Wiley, New York, 1997.